From www.bloodjournal.org by guest on April 20, 2017. For personal use only.

Loss of *Hspa9b* in zebrafish recapitulates the ineffective hematopoiesis of the myelodysplastic syndrome

Sarah E. Craven, Dorothy French, Weilan Ye, Frederic de Sauvage, and Arnon Rosenthal

Myelodysplastic syndrome (MDS) comprises a heterogeneous group of often-fatal hematopoietic stem cell disorders for which neither curative nor standard treatment exists. The complex karyotypes and multistep nature of MDS have severely restricted the identification of causative genetic mutations and thus limited insight into new and more effective therapies. Here we describe a zebrafish mutant crimsonless (*crs*) with a developmental blood defect that closely recapitulates the ineffective hematopoiesis of MDS including anemia, dysplasia, increased blood cell apoptosis, and multilineage cytopenia. By positional cloning, rescue, and morpholino knockdown experiments, we demonstrate that *crs* encodes a conserved mitochondrial matrix chaperone HSPA9B containing a glycine-to-glutamate substitution within the substrate-binding domain. This mutation compromises mitochondrial function, producing oxidative stress and apoptosis distinctly in blood cells. Thus, we identify an essential role for *Hspa9b* in hematopoiesis and implicate both loss of *HSPA9B* specifically and mitochondrial dysfunction generally in the pathogenesis of the MDS. (Blood. 2005;105:3528-3534)

© 2005 by The American Society of Hematology

Introduction

Myelodysplastic syndrome (MDS) comprises a heterogeneous group of clonal blood disorders characterized by ineffective hematopoiesis arising from dysplasia and accelerated apoptotic death of multipotential hematopoietic progenitors and their progeny.[1-3] These syndromes display significant clinical variability, and whereas some patients present solely with anemia and erythroid dysplasia, many develop fatal multilineage peripheral cytopenia or even progress to acute myeloid leukemia (AML).[1-3] Treatment options are limited, and the majority of patients with MDS die within 3 to 4 years.[1,2] Thus, the identification of genes whose loss or altered function produces defective hematopoiesis is critical for diagnosis, improved therapies, and prevention of neoplastic transformation.

Numerous chromosomal abnormalities have been linked to MDS, and although karyotypes are usually quite complex, interstitial deletions in the long arm of chromosome 5, del(5q), are prevalent in both de novo and therapy-induced cases.[4-8] A distinct subset of MDS, the 5q− syndrome, is characterized by good prognosis and deletions at chromosome 5q32 as the sole karotypic abnormality. In contrast, deletions at 5q31 are associated with more aggressive forms of MDS, often progressing rapidly to leukemia.[9,10] A critical deleted region (CDR) at chromosome 5q31 has been defined containing 9 candidate genes, including *HSPA9B*, but causative genes have yet to be identified.[10,11]

Compromised mitochondrial function is implicated in the pathogenesis of a wide variety of diseases, including MDS.[12,13] Structural abnormalities and iron accumulation are frequently found in the mitochondria of bone marrow cells from patients with MDS,[14,15] and these cells may display a proapoptotic profile, including activation of the mitochondrial death machinery and spontaneous release of cytochrome *c*.[16-18] Furthermore, mutations in the mitochondrial genome have been reported.[19] However, the exact role mitochondrial dysfunction plays in the ineffective hematopoiesis of MDS remains unclear.[13,20]

Hematopoiesis is well characterized in the zebrafish *Danio rerio* and demonstrates a high degree of conservation with mammalian counterparts.[21,22] Large-scale forward genetic screens have isolated zebrafish mutants at various stages in blood development[23,24] and several mutants model human hematopoietic diseases.[25,26] Here we present a characterization of the zebrafish developmental blood mutant crimsonless (*crs*). *crs* mutants are anemic at the onset of circulation and display defective blood cell differentiation followed by apoptosis and a reduction in erythrocytes, granulocytes, and hematopoietic progenitors. Furthermore, *crs* haploid insufficiency increased apoptosis specifically in adult hematopoietic progenitors. Thus the *crs* phenotype closely resembles the symptoms of MDS, and *crs* animals provide an additional valuable vertebrate model of these disorders.[27,28]

Using positional cloning, RNA rescue, and morpholino knockdown, we identified the mutated gene in *crs* as *Hspa9b* (mortalin/*mthsp70/GRP75*), a highly conserved, ubiquitously expressed, mitochondrial matrix chaperone. Mutant HSPA9B produces an increase in reactive oxygen species (ROS) and oxidative stress distinctly in blood cells. Thus our results demonstrate that *Hspa9b* is essential for proper hematopoiesis, and its loss and subsequent mitochondrial dysfunction in blood cells are sufficient to recapitulate characteristic symptoms of MDS.

Materials and methods

Fish stocks and maintenance

Fish were maintained and staged as described.[29,30] Embryos raised beyond 24 hours postfertilization (hpf) were treated with phenylthiourea (PTU; 0.003% wt/vol; Sigma, St Louis, MO) to prevent melanization.

From the Departments of Molecular Biology and Pathology, Genentech Inc, South San Francisco, CA; and Rinat Neuroscience, Palo Alto, CA.

Submitted March 22, 2004; accepted January 6, 2005. Prepublished online as *Blood* First Edition Paper, January 13, 2005; DOI 10.1182/blood-2004-03-1089.

Reprints: Sarah E. Craven or Frederic de Sauvage, 1 DNA Way, South San Francisco, CA 94080; e-mail: craven@gene.com or sauvage@gene.com.

The publication costs of this article were defrayed in part by page charge payment. Therefore, and solely to indicate this fact, this article is hereby marked "advertisement" in accordance with 18 U.S.C. section 1734.

© 2005 by The American Society of Hematology

From www.bloodjournal.org by guest on April 20, 2017. For personal use only.

Mapping and cloning

Fish carrying the *crs* mutation were out-crossed to WIK for positional cloning. Polymerase chain reaction (PCR) amplification of simple sequence length polymorphic (SSLP) genetic markers from gDNA of mutant versus heterozygous and wild-type (WT) *crs* embryos was used to establish linkage to linkage group 14 (LG14) between the markers z43267 and z26376. A chromosome walk was initiated from the closest marker z43267 (0.36 cM; 8 of 2239 recombinants) and single-stranded conformation polymorphism (SSCP) analysis was used to orient P1-derived artificial chromosomes (PAC) clones. Two PACs that displayed zero recombinants (0 of 2239) were identified. The PACs were sequenced, and both contained the complete coding region of the *Hspa9b* (GenBank accession no. 201326). A mutation in *Hspa9b* in *crs* embryos was demonstrated both by sequencing exons from gDNA and by reverse transcription-PCR (RT-PCR) of total RNA from mutant versus wild-type embryos. Full-length zebrafish *Hspa9b* was cloned by RT-PCR of total RNA from wild-type embryos using the TA cloning vector pCRII (Invitrogen, Carlsbad, CA).

Whole-mount in situ hybridization, o-dianisidine, acridine orange, and dihydrorhodamine 123 staining

Digoxygenin-labeled antisense RNA probes were hybridized at 68 to 70°C and developed with nitroblue tetrazolium (NBT) as described previously.[31] Probes for *gata1* and α and β-globins were generously provided by Dr Len Zon (Children's Hospital, Howard Hughes Medical Institute, Chevy Chase, MD). Probes for *alas2* and heme oxygenase-1 were isolated by RT-PCR and were TA cloned into pCRII (Invitrogen). Staining with o-dianisidine and labeling with acridine orange (AO) were performed as described.[24,32] Labeling with Mitotracker 580 and dihydrorhodamine 123 (Molecular Probes, Carlsbad, CA) was performed according to the manufacturer's protocol.

Histologic and TUNEL staining of embryonic blood cells and adult organs

Embryonic blood was isolated by cardiac puncture. Kidneys or liver from adult heterozygous and wild-type animals were dissected out and smeared onto glass slides. Wright-Giemsa staining was performed as previously described[25] and TdT-mediated dUTP nick-end labeling (TUNEL) analysis was performed using DeadEnd Fluorometric TUNEL System (Promega, Madison, WI) according to the manufacturer's protocol.

Whole-mount immunofluorescence

Embryos were dechorionated and fixed in 4% paraformaldehyde for 1 hour at room temperature or 4°C overnight. Embryos were equilibrated with 4 to 5 washes in −20°C methanol and stored overnight (minimum 1 hour) at −20°C, rehydrated through 50:50 methanol/phosphate-buffered saline with 0.1% Tween (PBST), washed once with dH_20, treated with −20°C acetone for 7 minutes, and washed with PBST. Embryos were blocked for 2 hours at room temperature in PBST, 5% normal goat serum (NGS), 2 mg/mL bovine serum albumin (BSA), 0.5% dimethyl sulfoxide (DMSO), and then incubated with 1° antibody (rabbit anti–active caspase-3, PharMingen [San Diego, CA], catalog no. 559565; rabbit antiphospho-histone H3, Upstate Biotechneology [Lake Placid, NY], catalog no. 06-570) in block overnight at 4°C. Embryos were washed in PBST and incubated 2 hours at room temperature with 2° cyanine 3 (Cy3) antibody in block and washed finally in PBST before mounting and imaging.

RNA and morpholino injections

Capped sense and antisense RNA was synthesized using the mMESSAGE mMACHINE kit (Ambion, Austin, TX) according to the manufacture's protocol from linearized $pCS2^+$ plasmids containing full-length *Hspa9b*. The sequence of the morpholino-modified antisense oligonucleotide (Gene Tools, Philomath, OR) targeting the zebrafish *Hspa9b* gene is as follows: 5′-TTGCCGTTCTCGACACAGACAACAT. RNA (~250 pg) or morpholinos (5-10 ng) was microinjected at the 1- to 4-cell stage. At 33 to 36 hpf, injected embryos were processed for o-diansidine staining.

RT-PCR

RNA was isolated from wild-type versus mutant embryos (Qiagen, Valencia, CA). Either 300 ng was used for Qiagen one-step RT-PCR according to the manufacturer's protocol and amplification products gel analyzed, or 25 ng for real-time RT-PCR (Applied Biosystems, Foster City, CA) using TAM/FAM-labeled probe/primer sets for *c-mpl* with *GAPDH* as a comparison and α_{e1}-globin as a positive control.

Image acquisition

Images were taken on either (1) a Leica dissecting microscope at 10 to 40 × with a Plan Apo objective (Leica Microsystems, Bannockburn, IL) in aqueous solution (Figures 1, 3D-E, and 5A-B); (2) a Nikon TE300 inverted microscope (Nikon, Kanagawa, Japan) with a × 60 oil objective with embryos mounted in Fluromount G (Figure 2A-D), or Plan Fluro × 20/0.45 air objective (Figures 2G-J and 4C-E), or Plan Fluro × 10/0.30 air objective (Figure 4A-B) in aqueous solution; or (3) a Nikon E800 upright microscope with Plan Apo × 40/0.95 air objective (Figures 2E-F, 4F, and 7), or Plan Apo × 20/0.75 air objective (Figures 4G-H, 5C-D, and 6) with embryos mounted in Fluromount G. All images were taken at room temperature with an RT Slider Spot camera (Diagnostic Instruments, Sterling Heights, MI) and acquired with Spot 3.5.2. version software for Windows. Subsequent manipulations were made using Adobe Photoshop (Adobe, San Jose, CA).

Results

crs mutants display a distinctive defect in blood development.

A single autosomal recessive allele of crimsonless (*crs*) was identified in a chemical mutagenesis screen for developmental mutants. *crs* embryos appeared visibly normal until approximately 33 hpf when light microscopy revealed hypochromic blood despite a normal number of cells in circulation. Analysis of erythroid hemoglobin content by whole-embryo staining with o-dianisidine confirmed the absence of hemoglobin in mutant animals compared to wild-type at both 33 hpf (Figure 1A-B) and 48 hpf (Figure 1C-F). However, overall blood development appeared normal up to 33 hpf as revealed by whole-mount in situ hybridization for *scl*, *gata2*, and *gata1* (Figure 1G-H and data not shown). Furthermore, mutant animals displayed normal expression of both α_{e1}- and β_{e3}-globin (Figure 1K-L and data not shown), and intravenous injection of iron-dextran failed to rescue hemoglobin production (data not shown). Thus, neither loss of blood formation, loss of globin chain expression, nor inadequate levels of circulatory iron account for the hypochromia of *crs* mutant embryos.

Accompanying the anemia, mutant blood cells failed to properly differentiate into mature erythrocytes. Hematoxylin and eosin staining at 33 hpf revealed significantly delayed development of red blood cells in *crs* mutant fish with large nuclei and basophilic cytoplasm characteristic of immature erythroblasts (Figure 2A-B). At 48 hpf mutant blood cells remained arrested at the erythroblast stage compared to the small, ellipsoid-shaped erythrocytes of wild-type animals (Figure 2C-D). Delayed blood cell development in mutant animals was also seen by Wright-Giemsa staining of isolated blood cells at 36 hpf (Figure 2E-F); however Prussian blue staining failed to detect the presence of ringed sideroblasts from altered iron utilization (data not shown). Further signs of dysplastic blood cells in mutant animals included the presence of binucleated cells (arrows in Figure 2B) and the failure to down-regulate expression of the early blood cell marker *gata1* (Figure 1I-J). Yet despite these defects, a small number of *crs* blood cells did produce hemoglobin by 48 hpf (Figure 1F). This late generation of hemoglobin was associated with an up-regulation of *alas2*, the

From www.bloodjournal.org by guest on April 20, 2017. For personal use only.

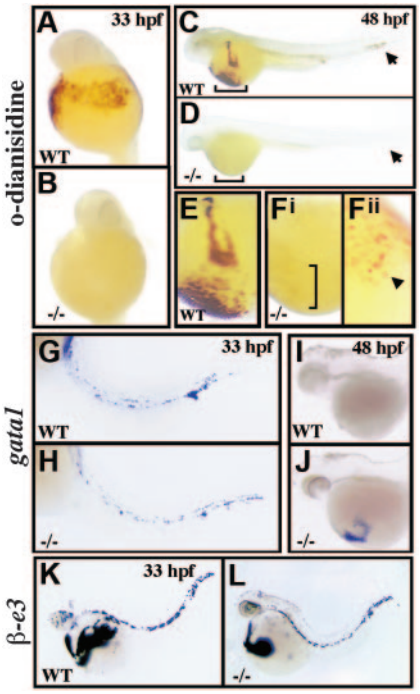

Figure 1. *crs* embryos are anemic despite normal blood specification. (A-F) Whole-mount o-dianisidine stain for hemoglobin in wild-type (WT) (A,C,E) and mutant (−/−) (B,D,F) embryos at 33 hpf (A-B) and 48 hpf (C-F). Arrows (C-D) indicate blood flow in the tail vessels. Blood flow over the yolk sac is bracketed (C-D) and shown higher magnification (E-Fi). A few o-dianisidine–positive cells over the yolk sac in mutant animals (bracket in Fi) are further magnified and indicated by an arrowhead (Fii). (G-L) Whole-mount in situ hybridization for *gata1* (G-J) and β_{e3} globin (L) at 33 hpf (G,H,K,L) and 48 hpf (I-J) in wild-type (G,I-K) and mutant (H,J,L) embryos.

rate-limiting enzyme in heme production (data not shown), suggesting that compensatory gene regulation allowed for the production of some functional hemoglobin in mutants.

In addition to anemia and dysplasia, the number of blood cells in circulation was also affected in mutant animals. Although normal at the beginning of development, the number of circulating blood cells began to decrease starting at around 36 hpf and by 38 to 42 hpf their numbers were on average one half to one fourth that of wild-type (Figure 2G-H). There was a reduction of cells flowing over the yolk sac and through the vessels including the caudal artery (Figure 2G-H and data not shown) with no signs of pooling or a decrease in the rate of blood flow. Subsequently, the number of blood cells in circulation either remained constant or in some individuals decreased further until death at approximately 72 hpf.

In contrast to the profound hematopoietic defect at 33 to 46 hpf, all other organ systems developed normally up to 48 hpf as revealed by molecular markers for vasculature, gut, and nervous system (data not shown). One exception was the head and eyes, which appeared stunted as early as 38 hpf. However, after 48 hpf all development appeared to halt, including further maturation of the musculature, fins, and internal organs, and most animals failed to survive past 72 hpf when the heart slowed and eventually stopped beating (data not shown).

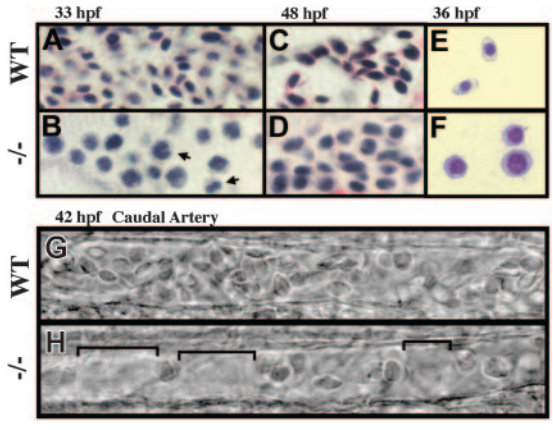

Figure 2. *crs* red blood cells fail to differentiate and are reduced in number. (A-D) Hematoxylin and eosin staining of blood cells from whole-mount wild-type (A,C) and mutant (B,D) embryos at 33 hpf (A-B) and 48 hpf (C-D). Binucleated cells were often observed (B, arrows). (E-F) Wright-Giemsa staining of isolated blood cells from wild-type (E) and mutant (F) embryos at 36 hpf. (G-H) Bright-field microscopy of blood cells in wild-type (G) and mutant (H) embryos at 42 hpf in the caudal artery with spaces between the reduced cell numbers in mutant animals bracketed (H).

Mutant *Hspa9b* is sufficient to account for the *crs* phenotype

To identify the gene responsible for defective hematopoiesis in *crs* embryos, we took a positional cloning strategy. Using polymorphic microsatellite markers, we mapped the *crs* mutation to LG14 between markers z43267 and z26376 (Figure 3A). A chromosome walk initiated from the closest marker z43267 (0.36 cM; 8 of 2239 recombinants) identified 2 partially overlapping PAC clones that displayed zero recombinants (0 of 2239 recombinants) and were sufficient to rescue the anemia in *crs* embryos (data not shown). The PACs were sequenced, and both contained the complete coding region of the ubiquitously expressed, mitochondrial matrix chaperone protein HSPA9B (Mortalin/mthsp70/GRP75). Sequence analysis of *Hspa9b* in *crs* mutants uncovered a point mutation leading to a glycine-to-glutamate substitution at position 492 (G492E) within the substrate-binding domain of HSPA9B (Figure 3B-C). This

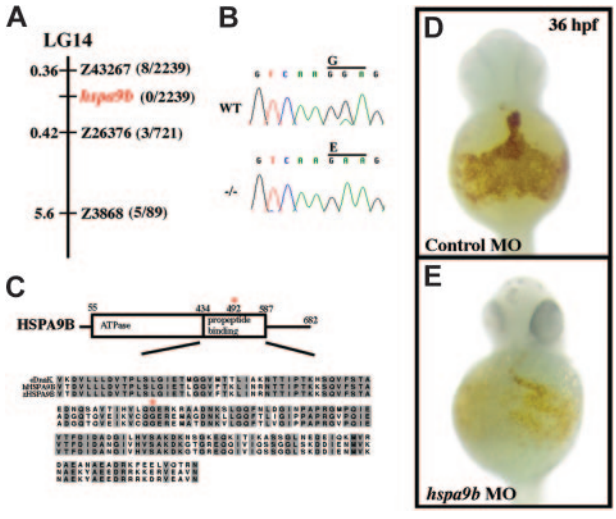

Figure 3. *crs* encodes a conserved mitochondrial matrix chaperone, HSPA9B. (A) The *crs* mutation is on linkage group 14 (LG14) between the polymorphic microsatellite markers z43267 and z26376. The distance between *crs* and each polymorphic marker is shown in centimorgans on the left, and the number of recombinants of 2239 meioses is on the right. No recombinants were found on 2 PACs that contain the entire zebrafish *hspa9b* gene. (B) ABI automated sequencer-produced chromatographs from wild-type (top) and mutant (bottom) mRNA. A G>A point mutation produces a glycine-to-glutamate conversion at amino acid 492 in zebrafish HSPA9B. (C) Domain structure of HSPA9B. HSPA9B has an N-terminal adenosine triphosphatase domain (amino acids 55-434) immediately followed by a propeptide-binding domain (amino acids 435-587) within which the G492E mutation lies (red asterisk). Underneath the domain map is an alignment of the propeptide-binding domains of zebrafish and human HSPA9B and *E coli*. DnaK chaperones with conserved residues in gray and the conserved glycine mutated in *crs* zebrafish marked with a red asterisk. (D-E) Whole mount o-dianisidine staining of embryos injected with control (D) or *hspa9b* (E) morpholino-modified antisense oligonucleotides (MO) at 36 hpf.

From www.bloodjournal.org by guest on April 20, 2017. For personal use only.

mutation was confirmed by RT-PCR of total RNA from mutant versus wild-type embryos. Zebrafish HSPA9B shares 84.8% identity and 89.4% similarity with human HSPA9B and 53.5% identity and 63.3% similarity with the *Escherichia coli* DnaK chaperone. A near-identical mutation in the conserved glycine at position 443 in DnaK completely abolishes propeptide binding, rendering the chaperone functionless.[33] Thus, *crs* likely represents a null allele of *Hspa9b*.

To verify that the mutation in *Hspa9b* is sufficient to cause the *crs* phenotype, we used both rescue and antisense morpholino knockdown experiments. Injection of capped RNA encoding wild-type HSPA9B rescued approximately 95% (53 of 56) injected mutant embryos. The blood of rescued animals was no longer hypochromic with o-dianisidine staining close to wild-type levels, and cytopenia did not occur up to 48 hpf (data not shown). No overexpression phenotype was observed in *Hspa9b*-injected embryos, and embryos injected with antisense RNA as a control were not rescued (0 of 44 injected; data not shown). Conversely, we inactivated zebrafish *Hspa9b* using antisense morpholino-modified oligonucleotides that targeted the 5′ untranslated region (UTR) and initiation methionine. Morpholino-injected embryos recapitulated the anemic phenotype observed in *crs* mutants, and approximately 80% of the injected animals showed decreased o-dianisidine staining compared to wild-type at 36 hpf (Figure 3D-E). Taken together these results provide strong support that the G492E mutation in HSPA9B is the cause of the *crs* phenotype.

Loss of *Hspa9b* recapitulates MDS

Human *HSPA9B* is located on the long arm of chromosome 5 within a CDR at 5q31 associated with MDS[10,11] and is thus a candidate for playing an important role in a subset of these blood disorders. Given that ineffective hematopoiesis including dysplasia, anemia, and a decline in circulating blood cells characterize both patients with MDS and *Hspa9b* mutant zebrafish, we further analyzed the blood defect of *Hspa9b* mutants to validate its relevancy to the human disease.

Although anemia is most typical of patients with MDS, it often occurs in conjunction with neutropenia or thrombocytopenia or both.[2] We therefore determined if multilineage cytopenia is present in *Hspa9b* mutant fish by examining myeloperoxidase-positive (*mpo*$^+$) cells of the neutrophil lineage, *L-plastin*-positive monocytes/macrophages, and CD41$^+$ thrombocytes.[34,35] *L-plastin*-positive myeloid cells, which initially originate outside the intermediate cell mass (ICM) over the anterior yolk sac,[34] were unchanged in number (data not shown), and similarly, despite failing to detect CD41 or the thrombopoietin receptor (*c-mpl*) by in situ, real-time RT-PCR revealed equivalent levels of *c-mpl* expression at 46 hpf in wild-type and mutant animals (data not shown). Yet in striking contrast, *mpo*$^+$ granulocytes, though unaffected at 18 to 24 hpf in the ICM (data not shown), are clearly reduced in number by 38 to 42 hpf in *crs* mutant embryos compared to wild-type (Figure 4). Thus our results differ from those of other zebrafish blood mutants with exclusive erythroid defects[25,26,34] and instead link the loss of *Hspa9b* not only with anemia but also with multilineage cytopenia.

The ineffective hematopoiesis of MDS is associated with increased apoptosis of hematopoietic stem cells and their progeny.[1-3] Accordingly, we analyzed whether blood cell apoptosis preceded cytopenia in *Hspa9b* mutant fish. An hour of incubation of live embryos with AO at 36 hpf labeled few dying cells in wild-type animals, and no blood cells were AO$^+$ (Figure 5A). By contrast, in mutant animals AO labeled circulating blood cells as well as immobile cells in the posterior ICM of the ventral tail

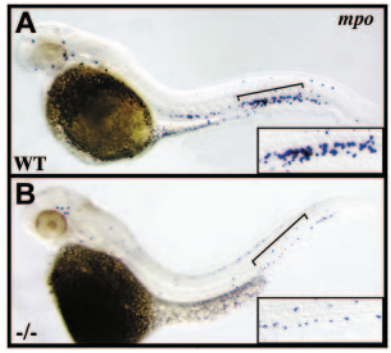

Figure 4. *crs* granulocytes are reduced in number. Whole-mount in situ hybridization for *mpo*$^+$ granulocytes at 42 hpf in wild-type (A) and mutant (B) embryos. Brackets indicate the tail regions shown at higher magnification in lower right corner of each panel.

(Figure 5B-E). Furthermore, an identical population of mutant cells was immunoreactive for activated caspase-3 (Figure 5F). Because the posterior ICM is a site where both hematopoietic progenitors[36] and phagocytic cells have been described,[37] these stationary cells may include both blood cells cleared from circulation as well as dying progenitors. Consistent with the latter, at 42 hpf *c-myb*$^+$ progenitors in the dorsal aorta were significantly reduced in mutant animals as compared to wild-type (Figure 5G-H). In contrast to the dramatic increase in cell death, the number of cells immunoreactive for phospho-histone H3, a marker of cell proliferation, was unchanged (data not shown). Cells in the eyes of mutant animals were the only other population that were positive for AO and activated caspase-3 (Figure 5B), and no additional cell populations labeled at 48 hpf or 72 hpf, indicating a lack of generalized cell death in mutant animals despite the lethal phenotype (data not shown).

In contrast to the hematopoiesis defect and lethality of homozygous *crs* embryos, a single wild-type copy of *Hspa9b* was sufficient to sustain embryonic development. Yet MDS manifest primarily later in life, so to determine whether haploid insufficiency affected adult definitive hematopoiesis, we analyzed kidneys from animals at 1 year of age for histologic abnormalities and apoptosis. Whereas Wright-Giemsa staining of kidney smears showed blood cells at all stages of development in approximately similar proportions in heterozygous versus wild-type animals (Figure 6A-B), TUNEL analysis demonstrated rates of apoptosis in heterozygous kidneys 3 to 5 times those seen in kidneys from wild-type clutchmates (Figure 6C-D). By contrast, the number of TUNEL$^+$ cells in smears from adult liver was similar regardless of genotype (data not shown). Thus *Hspa9b* haploid insufficiency specifically increased the susceptibility of developing blood cells to apoptosis.

Loss of *Hspa9b* produces oxidative stress preceding blood cell apoptosis

HSPA9B has been implicated in a number of cellular functions but most prominently as a chaperone for the transport, folding, and assembly of mitochondrial matrix proteins.[38-40] We thus looked for signs of mitochondrial dysfunction in blood cells from *Hspa9b* mutant animals. Normal mitochondrial respiration generates ROS, but when mitochondrial function is disrupted, levels of ROS can overwhelm the antioxidant capacity of cells, triggering oxidative stress and apoptosis.[41-45] To look for elevated ROS production, we incubated live animals with dihydrorhodamine 123 for approximately 1 hour. Starting at 34 hpf, dihydrorhodamine 123 specifically labeled blood cells in mutant embryos with maximal labeling

From www.bloodjournal.org by guest on April 20, 2017. For personal use only.

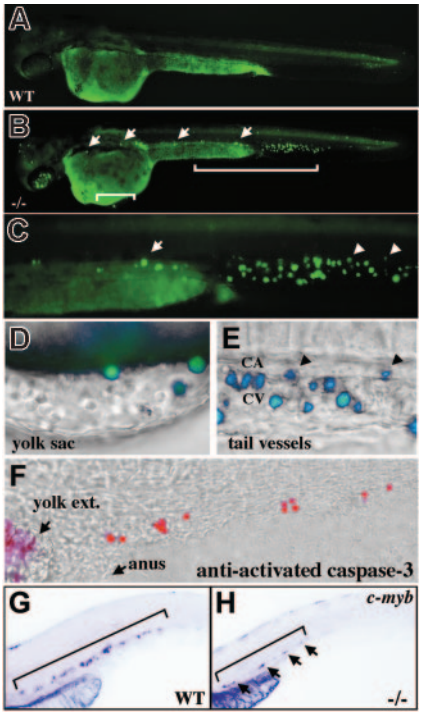

Figure 5. Apoptosis of *crs* blood cells. (A-E) Live wild-type (A) and mutant (B-E) embryos incubated with acridine orange at 36 to 38 hpf. The area bracketed in ventral tail (B) is shown at higher magnification (C) with far right arrow indicating the same labeled blood cell in panels B and C. Areas over the yolk sac (B) and in the ventral tail (C) are shown at higher magnification in panels D and E, respectively. Arrowheads indicate the same labeled blood cells in panels C and E. Fluorescent images overlay bright-field images (D-E) and labeled cells are surrounded by unlabeled blood cells over the yolk sac (D) and in the tail vessels; CA indicates caudal artery and CV caudal vein (E). (F) Whole-mount immunofluorescence on 36 hpf mutant embryos with an antibody against activated caspase-3 overlies a bright-field image in the ventral tail. The yolk extension (yolk ext) and anus are marked for orientation. (G-H) Whole-mount in situ hybridization for *c-myb*$^{+}$ stem cells at 42 hpf in wild-type (G) and mutant (H) embryos. Brackets delineate the positive progenitor population. Arrows in panel H mark positive cells in the mutant.

at 36 hpf (Figure 7A-B). Cells respond to increased ROS production by activating compensatory genes including the inducible isoform of heme oxygenase (*ho-1*).[41,46] In situ hybridization for *ho-1* at 30 hpf revealed sporadic expression in a small number of blood cells in approximately 80% of embryos regardless of genotype (data not shown). In contrast, at 36 to 38 hpf mutant

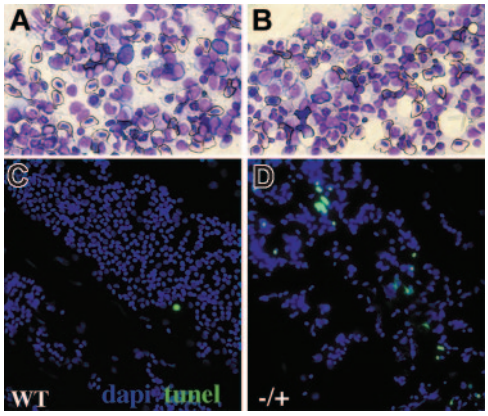

Figure 6. Increased blood apoptosis in adult *crs* heterozygotes. Kidney smears from wild-type (A,C) and heterozygous (B,D) adult *crs* animals showing hematopoietic progenitors and mature blood cells by Wright-Giemsa staining (A-B) or TUNEL (C-D) with nuclei shown by DAPI (4,6 diamidino-2-phenylindole; blue) and TUNEL (green) labeling dying cells.

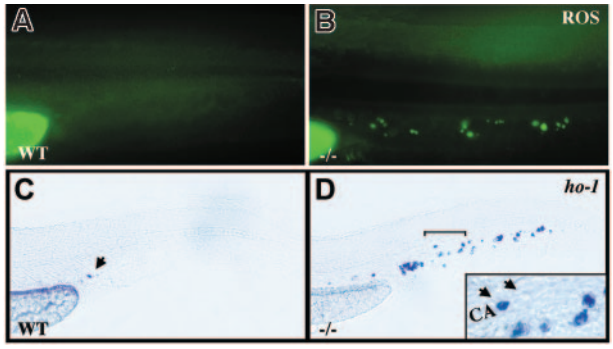

Figure 7. *crs* blood cells produce excess ROS and undergo oxidative stress. (A-B) Live wild-type (A) and mutant (B) embryos incubated with dihydrorhodamine 123 at 36 to 38 hpf. (C-D) Whole-mount in situ hybridization for heme oxygenase-1 (*ho-1*) at 36 to 38 hpf in wild-type (C) and mutant (D) embryos. A single cell in the tail vessels of the wild-type embryos is marked by an arrow in panel C. The region bracketed in panel D is shown at higher magnification (inset) with a *ho-1*$^{+}$ cell (arrow) next to an unlabeled cell (arrowhead) in the caudal artery (CA).

animals displayed a dramatic increase in the number of blood cells that expressed *ho-1* compared to heterozygous and wild-type animals (Figure 7C-D). Thus the loss of functional HSPA9B appears to produce blood cell death via oxidative stress.

Discussion

The zebrafish mutant *crs* displays a distinct hematopoietic defect including anemia, erythroid dysplasia, apoptosis of blood cells, and multilineage cytopenia. This phenotype closely resembles the characteristic ineffective hematopoiesis of the human blood disorders of MDS. Positional cloning, rescue, and gene knockdown analysis linked the *crs* phenotype to a point mutation in *Hspa9b*, a candidate causative gene in a subset of MDS patients,[10,11] that encodes a ubiquitous mitochondrial matrix chaperone. Thus we provide strong evidence that *Hspa9b* plays an essential role in blood cell development and independently implicate loss of *HSPA9B* and mitochondrial dysfunction in MDS pathogenesis.

HSPA9B is a member of the heat shock protein 70 family of chaperones. These chaperones are composed of 3 domains including a highly conserved C-terminal substrate-binding domain.[33] The crystallized substrate-binding domain of *E coli* DnaK revealed a β-sandwich containing the peptide-binding channel followed by 5 α helices.[47] Mutation of glycine 443 to aspartic acid was predicted to disrupt this structure and produced a complete loss of substrate binding, rendering the chaperone functionless.[33,47] The presence of the homologous G492E substitution in *crs* mutants strongly suggests that *crs* represents a null allele of *Hspa9b*.

HSPA9B is involved in the transport, folding, and assembly of proteins in the mitochondrial matrix including those involved in oxidative phosphorylation, metabolite biosynthesis, and protection from ROS.[12,48] HSPA9B also negatively regulates proteins involved in mitochondrial cell death including p53 and p66Shc, and its overexpression can immortalize cells and increase the lifespan in *Caenorhabditis elegans.*[40,49] Conversely, in yeast, *hspa9b (ssc1)* loss-of-function produces abnormal mitochondrial morphology, protein aggregation, and death[36,41,48] Mitochondrial function in *Hspa9b* mutant zebrafish appeared grossly normal as dyes that accumulate in functional mitochondria labeled mutant cells (S.E.C., unpublished results, June 2004). Rather, we find that *Hspa9b* mutant blood cells increased ROS production and induced expression of *ho-1* starting at 34 hpf. This delayed onset is common to

From www.bloodjournal.org by guest on April 20, 2017. For personal use only.

mitochondrial diseases,[12] and maternal contribution of wild-type HSPA9B may contribute to the delay. Oxidative stress was almost entirely restricted to blood cells and was accompanied by programmed cell death as indicated by labeling with AO and immunoreactivity for activated caspase-3. Furthermore, neither oxidative stress nor apoptosis became more generalized at 48 hpf, when development arrested, or at death around 72 hpf. Taken together, our results suggest that mitochondrial dysfunction in the absence of *Hspa9b* produces a mechanistically distinct defect in hematopoiesis that precedes general developmental arrest and thus provides insight into a human somatic blood cell disorder.

Many previously characterized zebrafish blood-specific mutants have defects restricted to the erythroid lineage.[23-26,34] And although anemia and erythroid dysplasia alone describe 2 of the 8 World Health Organization categories for MDS, the remaining disease classifications are characterized by bicytopenias or pancytopenias.[50] Here we demonstrate that mutant *Hspa9b* embryos have a reduction not only in red blood cells but also in *mpo*$^+$ myeloid cells. Thus, we link the loss of *Hspa9b* not just with anemia but also with multilineage cytopenia. In addition, we find that *c-myb*$^+$ hematopoietic progenitors were lost, suggesting that stem cell populations were affected by apoptosis as well. Definitive progenitors are observed in the posterior ICM and in the dorsal aorta as early as 24 hpf[36,37,51]; however, because it is unknown whether zebrafish hematopoietic stem cells continue to arise de novo, the failure of later stem cell populations to develop may also contribute to the reduction we observe in *c-myb*$^+$ cells.

Somatic chromosomal abnormalities are found in bone marrow cells from a high percentage of patients with MDS. Interstitial deletions in the long arm of chromosome 5 are common, and a CDR at 5q31 contains only 9 genes including *HSPA9B*.[11] Two AML cell lines with chromosome 5 deletions were previously analyzed for loss of heterozygosity in *HSPA9B* without success.[52] We did not detect a heterozygous embryonic phenotype; however, haploid insufficiencies can manifest later in life.[53] For example, heterozygous loss of superoxide dismutase *2* (*Sod2*), a critical component in mitochondrial ROS detoxification, results in an age-related oxidative stress and apoptosis in mice compared to the early lethality of the null.[54] Similarly we found that *Hspa9b* haploid insufficiency in zebrafish specifically increased the susceptibility of blood cell progenitors in the kidney to apoptosis. However, 1-year-old adult heterozygotes did not manifest obvious anemia or other characteristic symptoms of MDS, suggesting that further aging or alternatively loss of heterozygosity or other genetic lesions may be required.

Conversion of normal hematopoietic stem cells to an MDS state and ultimately a leukemic state is believed to be a multistep process requiring the accumulation of multiple genetic lesions.[2,13] Initial damage to the DNA of hematopoietic stem cells can arise de novo or as a result of exposure to toxic agents, including chemotherapeutic drugs or radiation. This primary event may precede the induction of well-recognized MDS-associated cytogenetic abnormalities and may act to increase both stem cell proliferation, contributing to clonal hematopoiesis, and susceptibility of the cell to further injury. Clonal selection may be then be assisted by alterations in the bone marrow microenvironment or immune dysregulation.[2] Subsequently, secondary genetic events such as a deletion at chromosome 5q and loss of *HSPA9B* could provide one route toward clonal evolution and the development of characteristic symptoms of MDS. And finally, further DNA damage may eventually lead to disruptions in the apoptotic response and leukemic transformation.[2,13] Deletions at 5q31 often result in rapid progression to leukemia.[9,10] Our finding that loss of functional HSPA9B results in high levels of ROS that can directly damage DNA and lead to further genetic lesions may help explain this poor prognosis.

Mutations in mitochondrial proteins and the mitochondrial genome are the primary defects in a number of diseases affecting organs with high energy demands including the nervous system and musculature.[41,55,56] Blood cells are less often affected; however, large deletions of mitochondrial DNA are associated with a rare congenital disorder, Pearson syndrome, which results in pediatric pancytopenia.[12,57] Also, transplantation of *Sod2*-deficient hematopoietic stem cells into wild-type mice resulted in a blood defect resembling sideroblastic anemia with oxidative damage and reduced survival of erythroid cells.[58] Our analysis of the *crs* zebrafish mutant indicates that a primary defect in a mitochondrial chaperone is sufficient to produce characteristic symptoms of the MDS blood disorders and implicates mitochondrial dysfunction in the pathogenesis of these syndromes.

Acknowledgments

The authors thank Drs Len Zon and Didier Stainier for reagents; Drs Barry Paw, Howard Stern, Leon Parker, and Erica Kratz for advice and technical assistance; and Maike Schmidt and T'Nay Pham for help and support.

References

1. Kurzrock R. Myelodysplastic syndrome overview. Semin Hematol. 2002;39(suppl 2):18-25.
2. Vergilio J-A, Bagg A. Myelodysplastic syndromes: contemporary biologic concepts and emerging diagnostic approaches. Am J Clin Pathol. 2003; 119:S58-S77.
3. Shimazaki K, Ohshima K, Suzumiya J, Kawasaki C, Kikuchi M. Apoptosis and prognostic factors in myelodysplastic syndromes. Leuk Lymphoma 2002;43:257-260.
4. Le Beau MM, Albain KS, Larson RA, et al. Clinical and cytogenetic correlations in 63 patients with therapy-related myelodysplastic syndromes and acute nonlymphocytic leukemia: further evidence for characteristic abnormalities of chromosomes no. 5 and 7. J Clin Oncol. 1986;4:325-345.
5. Pedersen-Bjergaard J, Phillip P, Larsen SO, Jensen G, Byrsting K. Chromosome aberrations and prognostic factors in therapy-related myelodysplasia and acute nonlymphocytic leukemia. Blood. 1990;76:1083-1091.
6. Smith SM, Le Beau MM, Huo D, et al. Clinical-cytogenetic associations in 306 patients with therapy-related myelodysplasia and myeloid leukemia: the University of Chicago series. Blood. 2003;102:43-52.
7. Bernasconi P, Alessandrino EP, Boni M, et al. Karyotype in myelodysplastic syndromes: relations to morphology, clinical evolution, and survival. Am J Hematol. 1994;46:270-277.
8. Mauritzson N, Albin M, Rylander L, et al. Pooled analysis of clinical and cytogenetic features in treatment-related and *de novo* adult acute myeloid leukemia and myelodysplastic syndromes based on a consecutive series of 761 patients analyzed 1976-1993 and on 5098 unselected cases reported in the literature 1974-2001. Leukemia. 2002;16:2366-2378.
9. Boultwood J, Fidler C, Strickson AJ, et al. Narrowing and genomic annotation of the commonly deleted region of the 5q− syndrome. Blood. 2002;99:4638-4641.
10. Liu TX, Zhou Y, Kanki, JP, et al. Evolutionary conservation of zebrafish linkage group 14 with frequently deleted regions of human chromosome 5 in myeloid malignancies. Proc Natl Acad Sci U S A. 2002;99:6136-6141.
11. Horrigan SK, Arbieva ZH, Xie HY, et al. Delineation of a minimal interval and identification of 9 candidates for a tumor suppressor in malignant myeloid disorders on 5q31. Blood. 2000;95:2372-2377.
12. Wallace DC. Mitochondrial diseases in man and mouse. Science. 1999;283:1482-1488.
13. Gattermann N. From sideroblastic anemia to the role of mitochondrial DNA mutations in myelodysplastic syndromes. Leuk Res. 1999;24:141-151.
14. Cohen AM, Alexandrova S, Bessler H, et al. Ultrastructural observations in bone marrow cells of 26 patients with myelodysplastic syndromes. Leuk Lymphoma. 1997;27:165-172.
15. van de Loosdrecht AA, Brada SJL, Blom NR, et al. Mitochondrial disruption and limited apoptosis

From www.bloodjournal.org by guest on April 20, 2017. For personal use only.

of erythroblasts are associated with high risk myelodysplasia. An ultrastructural analysis. Leuk Res. 2001;25:385-393.

16. Dror Y. The role of mitochondrial-mediated apoptosis in a myelodysplastic syndrome secondary to congenital deletion of the short arm of chromosome 4. Exp Hematol. 2003;31:211-217.
17. Boudard D, Sordet O, Vasselon, C, et al. Expression and activity of caspase 1 and 3 in myelodysplastic syndromes. Leukemia. 2000;14:2045-2051.
18. Tehranchi R, Fadeel B, Forsblom A-M, et al. Granulocyte colony-stimulating factor inhibits spontaneous cytochrome c release and mitochondria-dependent apoptosis of myelodysplastic syndrome hematopoietic progenitors. Blood. 2003;101:1080-1086.
19. Reddy PL, Shetty VT, Dutt D, et al. Increased incidence of mitochondrial cytochrome c-oxidase gene mutations in patients with myelodysplastic syndromes. Br J Haematol. 2002;116:564-575.
20. Shin MG, Kajigaya S, Levin BC, Young NS. Mitochondrial DNA mutations in patients with myelodysplastic syndromes. Blood. 2003;101:3118-3125.
21. Orkin SH, Zon LI. Genetics of erythropoiesis: induced mutations in mice and zebrafish. Annu Rev Genet. 1997;31:33-60.
22. Galloway JL, Zon LI. Ontogeny of hematopoiesis: examining the emergence of hematopoietic cells in the vertebrate embryo. Curr Topics Dev Biol. 2003;53:139-158.
23. Weinstein BM, Schier AF, Abdelilah S, et al. Hematopoietic mutations in the zebrafish. Development. 1996;123:303-309.
24. Ransom DG, Haffter P, Odenthal J, et al. Characterization of zebrafish mutants with defects in embryonic hematopoiesis. Development. 1996;123:311-319.
25. Brownlie A, Donovan A, Pratt SJ, et al. Positional cloning of the zebrafish *sauternes* gene: a model for congenital sideroblastic anaemia. Nat Genet. 1998;20:244-250.
26. Childs S, Weinstein BM, Mohideen M-APK, et al. Zebrafish *dracula* encodes ferrochelatase and its mutation provides a model for erythropoietic protoporphyria. Curr Biol. 2000;10:1001-1004.
27. Rithedech KN, Cronkite EP, Bond VP. Advantages of the CBA mouse in leukemogenesis research. Blood Cells Mol Dis. 1999;25;38-45.
28. Benito AI, Bryant E, Loken MR, et al. NOD/SCID mice transplanted with marrow from patients with myelodysplastic syndrome (MDS) show long-term propagation of normal but not clonal human precursors. Leuk Res. 2003;27:425-436.
29. Westerfield M. The Zebrafish Book. Eugene, OR: University of Oregon Press; 1993.
30. Kimmel CB, Ballard WW, Kimmel SR, Ullman B, Schilling TF. Stages of embryonic development of the zebrafish. Dev Dyn. 1995;203:253-310.
31. Guo S, Wilson SW, Cooke S, Chitnis AB, Driever W, Rosenthal A. Mutations in the zebrafish unmask shared regulatory pathways controlling the development of catecholaminergic neurons. Dev Biol. 1999;208:473-487.
32. Furutani-Seiki M, Jiang Y-J, Brand M, et al. Neural degeneration mutants in the zebrafish, *Danio rerio*. Development. 1996;123:229-239.
33. Burkholder WF, Zhao X, Zhu X, Hendrickson WA, Gragerov A, Gottesman ME. Mutations in the C-terminal fragment of DnaK affecting peptide binding. Proc Natl Acad Sci U S A. 1996;93:10632-10637.
34. Bennett CM, Kanki JP, Rhodes J, et al. Myelopoiesis in the zebrafish, *Danio rerio*. Blood. 2001;98:643-651.
35. Davidson AJ, Zon LI. The 'definitive' (and 'primitive') guide to zebrafish hematopoiesis. Oncogene. 2004;23:7233-7246.
36. Orkin SH, Zon LI. Genetics of erythropoiesis: induced mutations in mice and zebrafish. Annu Rev Genet. 1997;31:33-60.
37. Thompson MA, Ransom DG, Pratt SJ, et al. The *cloche* and *spadetail* genes differentially affect hematopoiesis and vasculogenesis. Dev Biol. 1998;197:248-269.
38. Craig E, Kramer J, Kosic-Smithers J. SSC1, a member of the 70kDa heat shock protein multigene family of *Saccaromyces cerevisiae* is essential for growth. Proc Natl Acad Sci U S A. 1987;84:4156-4160.
39. Kawai A, Nishikawa S, Hirata A, Endo T. Loss of the mitochondrial Hsp70 functions causes aggregation of mitochondria in yeast cells. J Cell Sci. 2001;114:3565-3574.
40. Wadhwa R, Taira K, Kaul SC. An Hsp70 family chaperone, mortalin/mthsp70/PBP74/Grp75: what, when, and where? Cell Stress Chaperones. 2002;7:309-316
41. Droge W. Free radical in the physiological control of cell function. Physiol Rev. 2002;82:47-95.
42. James AM, Murphy MP. How mitochondrial damage affects cell function. J Biomed Sci. 2002;9:475-487.
43. Lenaz G. Role of mitochondria in oxidative stress and ageing. Biochim Biophys Acta. 1998;1366:53-67.
44. Liu L, Trimarchi JR, Smith PJS, Keefe DL. Mitochondrial dysfunction leads to telomere attrition and genomic instability. Aging Cell. 2002;1:40-46.
45. Ueda S, Masutani H, Nakamura H, Tanaka T, Ueno M, Yodoi J. Redox control of cell death. Antioxid Redox Signal. 2002;4:405-414.
46. Ryter SW, Choi AMK. Heme oxygenase-1: molecular mechanisms of gene expression in oxygen-related stress. Antioxid Redox Signal. 2002;4:749-758.
47. Zhu X, Zhao X, Burkholder WF, et al. Structural analysis of substrate binding by the molecular chaperone DnaK. Science. 1996;272:1606-1614.
48. Orsini R, Migliaccio E, Moroni M, et al. The life span determinant p66Shc localizes to mitochondria where it associates with mitochondrial heat shock protein 70 and regulates trans-membrane potential. J Biol Chem. 2004;279:25689-25695.
49. Kang P-J, Ostermann J, Shilling J, Neupert W, Craig EA, Pfanner N. Requirement for hsp70 in the mitochondrial matrix for translocation and folding of precursor proteins. Nature. 1990;348:137-143.
50. Vardiman JW, Harris NL, Brunning RD. The World Health Organization (WHO) classification of the myeloid neoplasms. Blood. 2002;100:2292-2302.
51. Kalev-Zylinska ML, Horsfield JA, Flores MVC, et al. Runx1 is required for zebrafish blood and vessel development and expression of a human RUNX1-CBF2T1 transgene advances a model for studies of leukemogenesis. Development. 2002;129:2015-2030.
52. Xie H, Hu Z, Chyna B, Horrigan SK, Westbrook CA. Human mortalin (HSPA9): a candidate for the myeloid leukemia tumor suppressor gene on 5q31. Leukemia. 2000;14:2128-2134.
53. Traver D, Paw BH, Poss KD, Penberthy WT, Lin S, Zon LI. Transplantation and in vivo imaging of multilineage engraftment in zebrafish bloodless mutants. Nat Immunol. 2003;4:1238-1246.
54. Kokoszka JE, Coskun P, Esposito LA, Wallace DC. Increased mitochondrial oxidative stress in the *Sod2* (+/−) mouse results in the age-related decline of mitochondrial function culminating in increased apoptosis. Proc Natl Acad Sci U S A. 2001;98:2278-2283.
55. Parker JC. Commentary: human mitochondrial cytopathies. Ann Clin Lab Sci. 2000;30:159-162.
56. Schon EA, Manfredi G. Neuronal degeneration and mitochondrial dysfunction. J Clin Invest. 2003;111:303-312.
57. Rotig A, Colonna M, Bonnefont JP, et al. Mitochondrial DNA deletions in Pearson's marrow/pancreas syndrome. Lancet. 1989;1:902-903.
58. Friedman JS, Rebel VI, Derby R, et al. Absence of mitochondrial superoxide dismutase results in a murine hemolytic anemia responsive to therapy with a catalytic antioxidant. J Exp Med. 2001;193:925-934.

From www.bloodjournal.org by guest on April 20, 2017. For personal use only.

2005 105: 3528-3534
doi:10.1182/blood-2004-03-1089 originally published online January 13, 2005

Loss of *Hspa9b* in zebrafish recapitulates the ineffective hematopoiesis of the myelodysplastic syndrome

Sarah E. Craven, Dorothy French, Weilan Ye, Frederic de Sauvage and Arnon Rosenthal

Updated information and services can be found at:
http://www.bloodjournal.org/content/105/9/3528.full.html

Articles on similar topics can be found in the following Blood collections
Hematopoiesis and Stem Cells (3419 articles)
Neoplasia (4182 articles)

Information about reproducing this article in parts or in its entirety may be found online at:
http://www.bloodjournal.org/site/misc/rights.xhtml#repub_requests

Information about ordering reprints may be found online at:
http://www.bloodjournal.org/site/misc/rights.xhtml#reprints

Information about subscriptions and ASH membership may be found online at:
http://www.bloodjournal.org/site/subscriptions/index.xhtml

Blood (print ISSN 0006-4971, online ISSN 1528-0020), is published weekly by the American Society of Hematology, 2021 L St, NW, Suite 900, Washington DC 20036.
Copyright 2011 by The American Society of Hematology; all rights reserved.